Selective Cap Opening in Carbon Nanotubes Driven by Laser-Induced Coherent Phonons

Traian Dumitrică,[1,2] Martin E. Garcia,[1,3] Harald O. Jeschke,[4] and Boris I. Yakobson[2]

[1]*Institut für Theoretische Physik, Freie Universität Berlin, Berlin, Germany*
[2]*Center for Nanoscale Science and Technology, Rice University, Houston, Texas 77251, USA*
[3]*Advanced Materials Department, IPICYT, Camino Presa San José 2055, 78216, San Luis Potosí, SLP, Mexico*
[4]*Department of Physics & Astronomy, Rutgers University, Piscataway, New Jersey 08854, USA*

We demonstrate the possibility of a selective nonequilibrium cap opening of carbon nanotubes as a response to femtosecond laser excitation. By performing molecular dynamics simulations based on a microscopic electronic model we show that the laser-induced ultrafast structural changes differ dramatically from the thermally induced dimer emission. Ultrafast bond weakening and simultaneous excitation of two coherent phonon modes of different frequencies, localized in the spherical caps and cylindrical nanotube body, are responsible for the selective cap opening.

Many recent theoretical and experimental works have demonstrated that femtosecond laser pulses can induce irreversible ultrafast material modifications, in the form of solid-liquid [1–4] or solid-solid transitions [5–9]. Particularly interesting are ultrafast structural changes caused by the large amplitude of the coherent phonons induced by laser excitation, such as in Peierls-distorted Bi [5] or ferroelectric GeTe [6] materials. We show here for the first time the ability of coherent phonons to forcibly drive precise transformations in carbon nanotubes (CNTs). This finding is of a broader fundamental interest, including for the emerging field of nanotechnology, since it provides a unique way of manipulating lattice structures and shapes at the nanoscale level.

There are two distinct mechanisms through which an intense laser pulse can affect the structure of a molecule or a material: On a shorter time scale (~ 100 fs), the promotion of electrons to antibonding states immediately leads to a weakening of the bonds and the possibility of coherent atomic motion or nonthermal structural changes. By contrast, on a relatively longer time scale (>1 ps), as the energy of the photoexcited electrons is transferred into atomic thermal motion, structural changes occur in an uncontrolled manner.

At the nanoscale, the occurrence of thermal structural transformations is often mediated by high activation barriers and consequently requires a catalytic environment, or a high temperature usually achieved by pico- or nanosecond laser irradiation. So far, the potential of nonthermal transformations induced by femtosecond laser pulses has not been explored.

Here we describe the structural response of CNTs to femtosecond laser irradiation using quantum mechanical molecular dynamics (MD) simulations. Most remarkably, we find that the nonthermal response can induce a desired structural modification on a subpicosecond time scale, namely, a direct opening of the CNT's caps. By contrast, in a thermal regime we found CNTs to fragment by successive and stochastic dimer emission on a longer time scale.

To simulate the dynamical process of a laser-induced structural transition, we employ a nonadiabatic MD method combined with a density matrix formulation to describe the coupled dynamics of valence electrons and ionic cores [3,7]. In short, our treatment is based on a microscopic electronic Hamiltonian $H_{\mathrm{TB}} + H_{\mathrm{laser}}(t)$, where H_{TB} is a tight-binding (TB) Hamiltonian with hopping matrix elements and core-core repulsive terms that depend on interatomic distances $\{r_{ij}\}$, and $H_{\mathrm{laser}}(t)$ accounts for the coupling of the CNT's valence electrons to a time-dependent laser field of shape $E(t)$ and frequency ω. Our formulation assumes that the nondiagonal elements of the density matrix vanish rapidly in time due to dephasing effects. The equation of motion for the diagonal elements ρ_{ll} of the density matrix written in the H_{TB}'s eigenstate basis reads

$$\frac{\partial \rho_{ll}}{\partial t} = \frac{2}{\hbar^2} \mathrm{Re} \left\{ \sum_m g_{ml} \int_{t-\Delta t}^{t} dt' g_{lm}(\rho_{mm} - \rho_{ll}) \right\} + \frac{\partial \rho_{ll}}{\partial t} \bigg|_{coll}.$$

Here, $g_{lm} = \exp[i(\epsilon_l - \epsilon_m)t/\hbar] E(t) \cos(\omega t) x_{lm}$, with ϵ_l being eigenvalues of H_{TB}, is a matrix element of H_{laser} and, in turn, x_{lm} corresponds to the dipole matrix element between the TB states. Under the influence of an external e.m. field, the initial ground-state electronic distribution $\rho_{ll}^0 \equiv n_l(\mu_0, T_0)$ changes into a time-dependent nonequilibrium distribution $n_l(t)$. Further, the electronic thermalization term, taken as $\partial \rho_{ll}/\partial t|_{coll} \simeq [n_l(t) - n_l(\mu, T_e)]/\tau_{e-e}$, transforms the nonequilibrium electronic distribution into a Fermi-like function $n_l(\mu, T_e)$ within the relaxation time τ_{e-e}. Here, T_e and μ are the time-dependent electronic temperature and chemical potential, respectively. The total number of electrons remains constant during the simulation. This condition, together with

the equation describing energy absorption from the laser pulse [7], determines the values of T_e and μ. Finally, the forces $\mathbf{F}_i$ acting on the ith ion are determined as $\mathbf{F}_i(t) = -\nabla_i U(\{r_{ij}\}, \{n_l(t)\})$, where U is the time-dependent electronic free energy. U depends on interatomic distances $\{r_{ij}\}$, and its functional dependence is determined by $n_l(t)$.

With this model, in conjunction with the previously determined distance dependencies of the hopping matrix elements for carbon [10], we studied the response of both capped and "bulk"(treated with periodic boundary conditions) (10, 0)-CNT consisting of 200 atoms. The time step of $\Delta t = 0.1$ fs used in treating both electron and ion dynamics is small enough to capture the amplitude changes of the external e.m. field and to guarantee energy conservation when this e.m. field is absent. Like in graphite, τ_{e-e} was taken to be 10 fs [3].

Let us analyze now the nonthermal CNT fragmentation. Figure 1 shows sequences [11] of the CNT response following absorption of 2 eV/atom from a 10 fs laser pulse of Gaussian shape [12]. As a result of the laser excitation, approximately 8% of valence electrons are promoted into antibonding states. A brief analysis of the partial Mulliken charges left below the Fermi level revealed that energy absorption is approximately uniform over a CNT surface (caps and body). Additionally, variations of the full Mulliken atomic charges are negligible during fragmentation. There are two remarkable features in the simulation of Fig. 1: The first is a simultaneous release of both hemispherical caps at $t = 150$ fs after the laser peak. Second is the conservation of the cylindrical body, which is preserved for the next 2 ps. Here, the
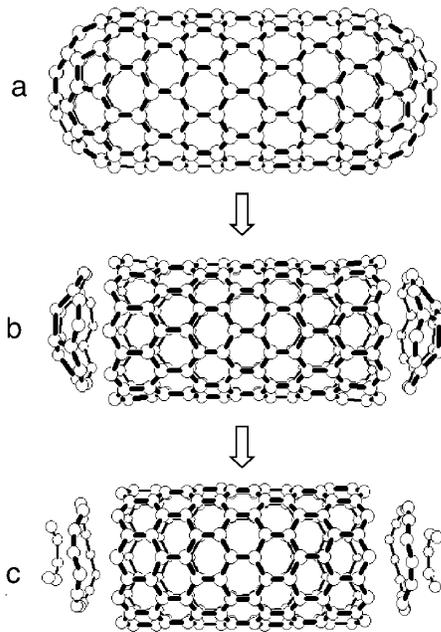

FIG. 1. Response of a (10, 0)-CNT leading to cap expulsion. The pictures were selected at (a) 0, (b) 150, and (c) 180 fs, measured from the peak time of a 10 fs laser pulse of central frequency 1.9 eV. The average absorbed energy is 2.0 eV/atom.

incoming-photon energy was 1.9 eV and, for a clear differentiation from the thermal component, the laser pulse was applied to the CNT at just above 0 K (more precisely 8 K, as obtained by evolving a slightly off-equilibrium CNT configuration). However, we confirmed its fundamental nature by reproducing the cap opening with samples initially thermalized to $T = 300$ K, for different incoming-photon energies and for a broad range of laser intensities. We have also found cap opening in (5,5) armchair tubes. What is the origin of the nonthermal selective photofragmentation?

As a first step to answer this question let us first analyze solely the laser response of the cylindrical CNT's body, treated with periodical boundary conditions over a deformable cell. The last feature is appropriate since CNTs can be entirely contained in the lateral extension of a typical laser spot. The most salient feature of the CNT response to a femtosecond light pulse is an impulsive excitation of the radial breathing mode (RBM), as we observed from the computer visualization of the motion in real space, or from test studies of vibrational power spectra. The driving mechanism is a displacive excitation [13]: Since the electronic configuration $n(\mu, T_e)$ is not the ground-state one, the atomic positions are no longer in equilibrium. As a result, the atoms move towards the new minimum and oscillate around it. To rationalize the impulsive displacement observed in the MD simulations, we have next performed simulated annealing towards a 0 K lattice temperature while maintaining the $n_l(\mu, T_e)$ electronic distribution at high T_e, with the aim of precisely obtaining the new minima. For the case of bulk CNT we have obtained that electronic temperatures of 15 000, 20 000, and 25 000 K lead to length and diameter increases of 1, 2, and 4%, respectively [14]. Above a threshold excitation, the new minimum does not exist and the material will fragment. In the case of bulk (10, 0)-CNT, our MD simulations with 10 fs pulses indicate a lower than graphite [3] absorbed energy threshold of $E_{\text{bulk}} = 2.8$ eV/atom, corresponding to a 10% promotion of valence electrons into antibonding states. We note that the joining of the (10, 0)-CNT's caps forms the C_{60} molecule, whose fragmentation threshold was previously found at $E_{C_{60}} = 2.1$ eV [7]. Therefore, the existence of an absorbed energy range for which the CNT's caps fragment selectively seems likely. We also note that the decreasing values of the ultrafast ablation thresholds in the graphite layer, CNT, and C_{60} correctly reflect the weakening of C-C bonding with curvature.

For the capped (10, 0)-CNT, the displacive excitation will produce two coherent phonon modes, localized in the spherical caps and cylindrical body. To monitor these oscillations, Fig. 2 displays the temporal evolution of $R_s(t)$ and $R_t(t)$, the average spherical cap and tubular radii. The relatively low laser absorbed energy of 1 eV/atom insures that the original connectivity is preserved. We observe that the two oscillation frequencies are different, and in fact correspond to the individual
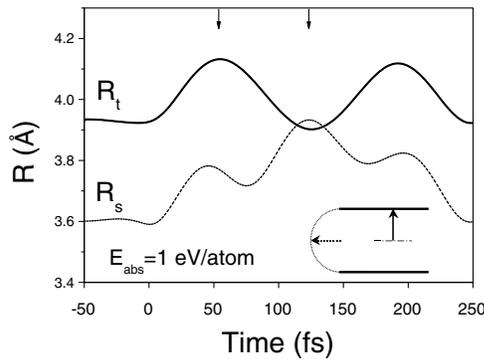
FIG. 2. Time evolution of $R_s(t)$ and $R_t(t)$, the CNT's cap (dashed line) and cylindrical part (full line) averaged radii (shown in the insert), at a subthreshold absorbed energy of 1.0 eV/atom. Time is measured from the peak time of the 10 fs pulse. Down arrows mark the cap opening times corresponding to the two discussed mechanisms.

RBM of C_{60} ($\omega_s = 500$ cm^{-1}) and $(10,0)$-CNT ($\omega_c = 300$ cm^{-1}). The two coherent phonons seem decoupled, most likely due to the predominantly perpendicular oscillation directions. This result agrees with the experimental CNT vibrational spectra, where a distinct RBM peak was attributed to the caps [15].

A brief analysis of Fig. 2 shows that both the caps and the CNT's body start expanding *in phase*, reaching their maximum amplitude after 50 fs (measured from the laser peak time). The initial correlation is not preserved due to different characteristic RBM frequencies and after 100 fs the two oscillations become *out of phase*. To place this behavior in a broader context, we note that, although RBM frequencies are curvature dependent, the fraction ω_s/ω_t remains constant [16] (~ 1.6 for graphite) for any spherical and cylindrical shell pair with same radius and made of the same material. Since the RBM frequencies do not depend on chirality [17], we infer that the behavior shown in Fig. 2 remains qualitatively true for any capped CNT, along with the selective cap opening mechanisms discussed next.

Based on the above RBM oscillation analysis for lower laser intensities we are now in the position to understand the selective CNT cap opening, occurring at intensities that more severely weaken the C-C bonding. The simulations at absorbed energies just below E_{bulk}, in the range of 2.2–2.8 eV/atom, indicated that the CNT caps are dramatically affected and cannot sustain the initial displacive excitation. Consequently, a selective cap photo-fragmentation occurs while the two oscillations are still *in phase*, starting at the first down arrow of Fig. 2. For the lower absorption energy range of 1.8–2.2 eV, selective cap opening still occurs by a different mechanism: Although the caps are strong enough to survive the initial simultaneous expansion, the *out of phase* oscillation, marked by the second down arrow in Fig. 2, subjects the cap-body interface region to an increased strain. In conjunction with the C-C bond weakening due to the

promotion of about 8% of valence electrons into anti-bonding states, the direct cap release is attained, as shown in Fig. 1. Finally, below this range no structural changes have been observed during the 2 ps simulation time since the C-C bonds remain strong enough to sustain the two coherent oscillations.

We can conclude that in the nonthermal regime, laser manipulation of the CNT structure is possible through an impulsive excitation of RBMs and a coherent phonon oscillation on the weakly bound system. Such a transformation occurs with a fairly cold lattice, as can be seen from Fig. 3, which shows the instantaneous temperature of the capped tube and tube only at $E_{abs} = 2.0$ eV. Because of the displacive excitation, during the first 100 fs after irradiation the ions acquire a large amount of kinetic energy, reaching a maximum of $T \simeq 800$ K, which is far below the CNT's melting point. Following the cap release, after ~ 200 fs, the tube stabilizes at $T \simeq 300$ K and it is clear that on the subpicosecond time scale no further structural damage occurs. However, it is important to realize that the CNT is still in a nonequilibrium state and could suffer subsequent structural changes. Of course, only a fraction of the electronic absorbed energy will be transferred to the lattice and the final T is determined mainly by the competition between the *e-ph* transfer and the hot electron transport. The prospects of subsequent melting or thermally activated processes are weak if the CNTs are placed on a substrate or in solution. This is because even metallic CNTs (of typical armchair orientation) are characterized by a weak *e-ph* coupling, which corresponds to a long mean free path l_{e-ph} exceeding 1 μm or scattering time τ_{e-ph} of 15 ps [18]. (For comparison, the *e-ph* transfer in graphite occurs in a few hundred femtoseconds.) Suppression of *e-ph* transfer by a faster energy coupling into a substrate is likely, and has already been observed in C_{60} films on silicon surfaces [19].

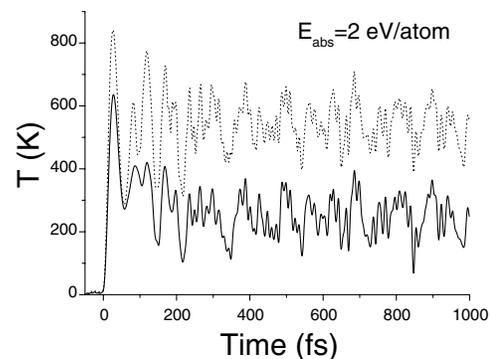Finally, in order to show that the nonequilibrium CNT fragmentation differs dramatically from thermally

FIG. 3. Time dependence of the instantaneous ionic temperature, proportional to $\sum_{i=1}^{N} v_i^2(t)$, where $v_i^2(t)$ is the square of the norm of the ionic velocity at time t. The i index runs over the total number of atoms (dotted line) or only over the atoms belonging to the CNT's body (full line).
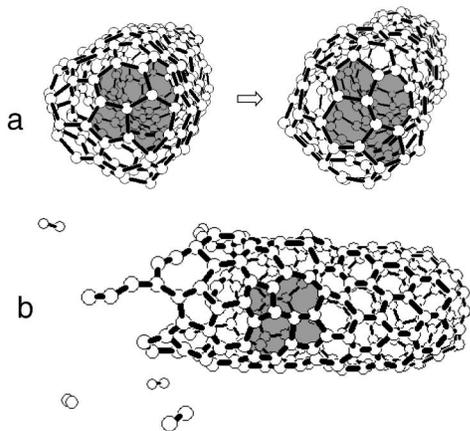
FIG. 4. Thermal fragmentation of capped CNT at $T = 5400$ K proceeds with (a) formation of a SW defect in the cap region, which transforms the initial 5|6|6|6 arrangement (left) into a strained 6|5|7|5 configuration (right). (b) Melting occurs at the defect by successive emission of C_2 fragments. Another SW defect which emerged 1 ps after the first one is visible on the CNT body.

induced structural changes, we performed MD simulations using the same TB model but replacing the laser excitation by a thermal one. Thus, we considered a $(10, 0)$-CNT capped geometry in thermal equilibrium, i.e., with lattice and electrons being at the same temperature T. T was increased by 400 K at 2 ps intervals.

Because of the remarkable C-C bond strength, we expect CNTs to exhibit structural changes only at quite elevated T for the time scale accessible by MD simulations. Figure 4(a) shows the first observed defect event as T reached 5400 K, a Stone-Wales (SW) $90°$ bond rotation occurring in one of the CNT caps, followed by another SW defect on the CNT body. As the simulation continues, the area around the defective cap exhibits signs of failure, as intuitively expected [20]. The structure depicted in Fig. 4(b), obtained after 3 ps from the formation of the initial SW defect, shows a dramatic CNT failure by a successive dimer release. One notes that the SW defect is the lowest energy defect in CNTs, and therefore the most favorable thermodynamically. The temporal sequence of SW occurrence appears to agree with the *ab initio* SW activation data [21], which indicate a lower barrier for spherical geometry. Finally, failure by a C_2 shredding mechanism concurs to the existing experimental observations on fullerene thermal fragmentation [20].

In conclusion, we studied the response of capped CNTs to ultrafast laser pulses. Selective CNT cap opening was attained over a large absorbed energy range. Our result may have a significant impact since the opening of the CNT caps with little loss of material is a challenging technological issue [22], motivated, for example, by the perspective of nanoconfinement of molecular species inside a CNT's cavity. In the quest of growing longer CNTs, ultrafast laser pulses could also be used to periodically remove the unwanted caps which prematurely terminate CNTs.

[1] P. Saeta *et al.*, Phys. Rev. Lett. **67**, 1023 (1991).
[2] P. L. Silvestrelli and M. Parrinello, J. Appl. Phys. **83**, 2478 (1998).
[3] H. O. Jeschke, M. E. Garcia, and K. H. Bennemann, Phys. Rev. Lett. **87**, 15003 (2001).
[4] T. Dumitrică and R. E. Allen, Phys. Rev. B **66**, 081202 (2002).
[5] K. Sokolowski-Tinten *et al.*, Nature (London) **422**, 287 (2003).
[6] M. Hase *et al.*, Appl. Phys. Lett. **83**, 4921 (2003).
[7] H. O. Jeschke *et al.*, Chem. Phys. Lett. **352**, 154 (2002).
[8] A. Cavalleri *et al.*, Phys. Rev. Lett. **87**, 237401 (2001).
[9] T. E. Glover *et al.*, Phys. Rev. Lett. **90**, 236102 (2003).
[10] C. H. Xu *et al.*, J. Phys. Condens. Matter **4**, 6047 (1992).
[11] See EPAPS Document No. E-PRLTAO-92-020409 for a visualization of the structural response of a (10,0) carbon nanotube to a femtosecond laser pulse. A direct link to this document may be found in the online article's HTML reference section. The document may also be reached via the EPAPS homepage (http://www.aip.org/pubservs/epaps.html) or from ftp.aip.org in the directory /epaps/. See the EPAPS homepage for more information.
[12] This corresponds to a fluence of $F = 0.26$ J/cm^2, assuming a 50 nm laser penetration depth, along with the reflectivity of graphite [3]. Note that multiphoton absorption is still weak at the resulting pulse intensity of 2.6×10^{13} W/cm^2, according to experimental data on C$_{60}$: M. Tchaplyguine *et al.*, J. Chem. Phys. **112**, 2781 (2000).
[13] H. J. Zeiger *et al.*, Phys. Rev. B **45**, 768 (1992).
[14] Variations in CNT dimension at changed chemical potential caused by charge injection have been previously reported. See R. Baughman *et al.*, Science **284**, 1340 (1999).
[15] P. V. Huong *et al.*, Phys. Rev. B **51**, 10 048 (1995).
[16] $\omega_s/\omega_t = 2\sqrt{(\lambda + \mu)/(\lambda + 2\mu)}$, where λ and μ are the Lamè material coefficients. See S. Erdin and V. L. Pokrovsky, Int. J. Mod. Phys. **15**, 3099 (2001).
[17] K. N. Kudin *et al.*, Phys. Rev. B **64**, 235406 (2001).
[18] G. Moos *et al.*, J. Nanosci. Nanotech. **3**, 145 (2003).
[19] L. Bolotov and T. Kanayama, Phys. Rev. B **68**, 033404 (2003).
[20] S. C. O'Brien *et al.*, J. Chem. Phys. **88**, 220 (1988).
[21] G. E. Scuseria, Science **271**, 942 (1996).
[22] P. M. Ajayan *et al.*, Nature (London) **362**, 522 (1993).